

High shear melt-processing of fiberglass-reinforced poly(trimethylene) terephthalate composites

Jennifer Krystyna Lynch

Rutgers University, Materials Science and Engineering Department, 607 Taylor Road, Piscataway New Jersey 08854

Correspondence to: J. Lynch (E-mail: jklynch@rci.rutgers.edu)

ABSTRACT: As the demand for polymer-matrix composites (PMC) expands in order to replace traditional materials, processing of the PMC is increasingly vital, as the morphology and properties are processing dependent. Typically, thermoplastic PMCs are processed in at least two heat-intensive steps, including a pre-compounding step in order to achieve good mixing followed by a part fabrication step. The key aim of this study is to prepare a fiberglass-reinforced poly (trimethylene terephthalate) (FG-PTT) composite using a one-step, high shear melt-processing method that achieves both compounding and part fabrication. The morphology, thermal properties, and mechanical properties are characterized to determine the effect of FG reinforcement on this renewable biopolymer. This novel method produces a FG-PTT composite with superior mixing and tensile strength, as well as enhanced toughness, in one processing step, reducing polymer degradation and fiber attrition, as well as, time, energy, and cost requirements. © 2015 Wiley Periodicals, Inc. *J. Appl. Polym. Sci.* **2015**, 132, 42714.

KEYWORDS: thermoplastics; composites; molding; morphology; mechanical properties

Received 6 February 2015; accepted 10 July 2015

DOI: 10.1002/app.42714

INTRODUCTION

Thermoplastic polymer matrix composites (PMC) are sought to replace traditional materials, like glass, aluminum, steel, and concrete, in a wide array of applications, offering many benefits, including variability in processing and part fabrication. The final part properties are directly dependent upon the processing method and resultant morphology. Dispersing and distributing pigment, modifiers, fillers, particles, reinforcing agents, and other various compounds within a thermoplastic matrix are difficult.

Twin screw extrusion is commonly used for compounding in order to achieve good mixing followed by a second processing step, like injection molding, for part fabrication. However, subjecting the polymer to multiple processing steps has its disadvantages, including every time a polymer is subject to heat and shear forces there is potential for degradation, chemical or otherwise; multiple processing steps have been found to coarsen the morphology of a previously well mixed system¹; mechanical properties are dependent upon morphology; particles may tend to agglomerate during extrusion; and particle aspect ratio reduction because of attrition. Additionally, multiple processing steps increase energy usage, manufacturing costs, coordination steps, and time. However, single screw extrusion with new mixing element designs offers several advantages over twin screw extrusion,² which has changed the function of single screw extrusion from only plasticating to both plasticating and mix-

ing.³ For homogeneity, dispersive mixing followed by distributive mixing is optimal.⁴

After years of experimental observation, the authors discovered a high compounding mixer (HCM) for use with single screw extrusion, which provides enhanced mixing and toughness without sacrificing modulus and strength.^{5,6} For example, processing an immiscible polymer blend (IMPB) of polystyrene (PS) and high density polyethylene (HDPE) using this HCM screw design results in a fine morphology of good mixedness (approximately 1 μm HDPE domains) and fractures at 12% strain, as shown in Figure 1.⁷ Conversely, processing the same materials and concentration with a typical, commercially used mixer in the screw design results in a more coarse-grained structure (approximately 10 μm HDPE domains) with similar modulus and strength but fractures at only 5% strain, as shown in Figure 1. Thus, the authors incorporated HCMs into the screw design of an injection molding machine in order to compound and fabricate parts in a one-step, novel injection molding process.

Along with processing improvements, polymer selection for the matrix of a PMC determines its properties and applications. Poly trimethylene terephthalate (PTT), is a linear aromatic polymer with three methylene groups in the backbone; belongs to the polyester family, along with polyethylene terephthalate (PET), and poly butylene terephthalate (PBT); and has engineering-grade properties. PTT is synthesized from 1,3-propanediol (PDO) with

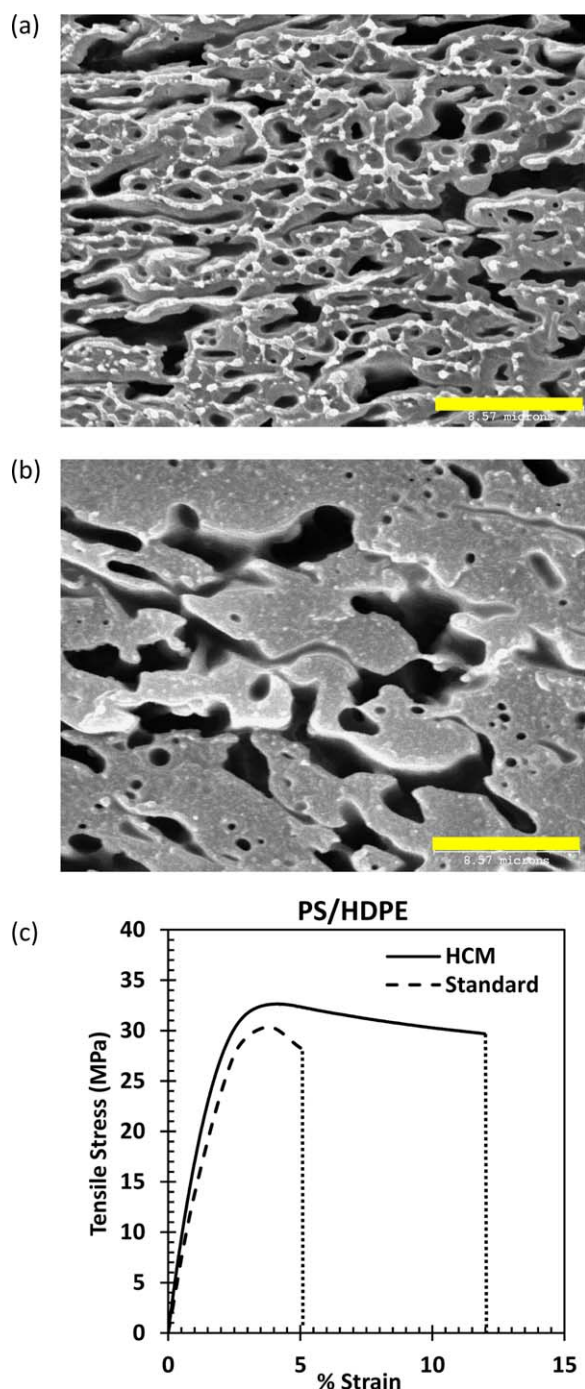


Figure 1. PS/HDPE processed using single screw extrusion: (a) SEM micrograph at 8.57 μm scale produced with HCM, (b) SEM micrograph at 8.57 μm scale produced with standard mixers (PS phase was leached with toluene from the cryogenically fractured surface for better contrast and appears black), and (c) Corresponding tensile stress-strain curves. [Color figure can be viewed in the online issue, which is available at wileyonlinelibrary.com.]

either terephthalic acid or dimethyl terephthalate, followed by polymerization. Production of PDO is possible from petrochemical sources, as well as, from renewable resources via biological processes.⁸ Thus, PDO may be bio-sourced for the fermentation process; however, PTT is not bio-degradable. The chemical struc-

ture of PTT is shown in Figure 2. The crystallization of PTT has been widely studied, including the crystal structure,^{9,10} morphology,¹¹ crystallization kinetics,^{12–14} and melting behavior.¹⁵ The mechanical properties and structure,^{14,16} as well as aging effects on the mechanical and thermal properties and structure,¹⁷ have been investigated. Its beneficial properties, similar to high-performance PBT, are derived from a unique, semi-crystalline molecular structure featuring a pronounced "kink".

The initially intended application of PTT was in the textile industry as a fiber because of its superior resiliency and chemical resistance.^{17–19} PTT has found new opportunities in carpet, textile, film, packaging, and engineering thermoplastics^{14,20} markets because of (1) breakthroughs in PDO synthesis that has made PTT available in industrial quantities¹⁴ and (2) efforts since the 1990s by DuPont to develop cost-effective production, processing, and applications of PTT.⁸

Many studies compare PET, PBT, and PTT, since they potentially compete for the same engineering-grade thermoplastic market.^{8,14,16,20,21} The crystallization rate from fastest to slowest for these three polyesters is PBT, PTT, and PET, each one having a crystallization rate an order of magnitude higher than the other.¹² The crystallization rate of PTT and short-comings of PET and PBT suggest that PTT may be best suited for injection molding applications.^{12,14} PTT offers similar physical properties of PET (including strength, stiffness, toughness, and heat resistance), dimensional stability, electrical insulation, chemical resistance, and better processability than PET.¹⁴ PTT "is a viable candidate for engineering structural applications, which are presently addressed by nylon 6/6, PET, and PBT."²⁰

To improve properties of polyesters, fiberglass (FG) reinforcement is commonly used to provide a high-end engineering thermoplastic composite that may compete more directly with thermosets and high temperature thermoplastics in very demanding applications. There are a small number of studies that have investigated FG-reinforced PTT, with comparisons to FG-reinforced PET and FG-reinforced PBT.^{14,20,22} FG-reinforced PTT had the highest stiffness and toughness relative to FG-reinforced PET and FG-reinforced PBT and had superior tensile strength and heat deflection temperature relative to FG-reinforced PBT.²⁰

The aim of this work was to develop a novel, one-step melt-processing method to produce a FG-PTT PMC at various concentrations and characterize the mechanical and thermal properties, as well as the morphology. This novel method is a patent-pending, one-step processing method that accomplishes both compounding and part fabrication and allows reinforcing agents, powder or liquid pigments, and fillers to be added with the bulk polymer

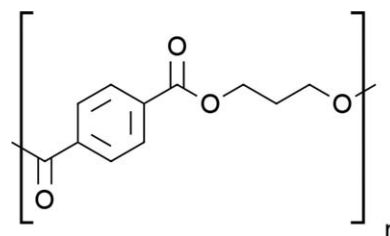


Figure 2. Chemical structure of PTT.

resin directly into an injection molding machine with a novel screw design in the plasticating unit.²³ Advantages of processing the FG-PTT PMC by this novel method include: (1) a better final part because of good mixing, less fiber attrition during processing, and less heat history to the polymer, (2) a less expensive final part because of elimination of the costly compounding step, (3) energy and cost savings, and (4) easier materials handling and logistics since only basic ingredients are necessary to store just prior to final part manufacture, rather than precompounded and proprietary mixtures.

EXPERIMENTAL

Materials

Two components were used for this experimental mixing study, including FG and polytrimethylene terephthalate (PTT). No processing aids were used to promote fiber–matrix adhesion. The FG (manufactured by Eager Polymers) is typical micron-sized chopped strand E Glass ($d = 20\ \mu\text{m}$, $L = 4\ \text{mm}$) with a silane coating appropriate for mixing with polyester resins. PTT (manufactured by DuPont), contains 20–37 weight % renewably sourced material and has a melting temperature of approximately 227°C.

Processing

Prior to melt-processing, PTT was dried at 150°C for about 12 hours. FG-PTT components were dry-blended in concentrations of 0, 10, 15, 20, and 30 wt % FG in PTT. Dry-blended components were added directly to the hopper of a Negri Bossi V55–200 IM machine with a novel screw design, including two HCM elements and melt-processed at 100 RPM, and processing temperatures for zones 1, 2, 3, and the nozzle were 246°C, 242°C, 240°C, and 240°C, respectively. The stainless steel mold temperature was not controlled and was approximately room temperature. Standard ASTM D638 Type 1 tensile specimens and D256 impact specimens with cross-sectional dimensions of approximately 3.4 mm by 12.5 mm were produced. After processing, specimens were conditioned at room temperature prior to mechanical property testing, according to ASTM D 638 and D 256.

Characterization

Morphology Analysis. A Hitachi S-2600 scanning electron microscope (SEM) was used for morphology analysis. SEM samples were prepared by cryogenic fracture at liquid nitrogen temperatures. The fractured specimens were mounted on aluminum studs and gold coated. The specimens were fractured parallel and perpendicular to the extrusion axis to show fiber orientation and distribution.

Thermal Property Test. Thermal properties were determined using a TA Instruments Q1000 Differential Scanning Calorimeter (DSC) using a heat/cool/reheat method over a temperature range from 0°C to 250°C at a rate of 10°C/min under a blanket of dry nitrogen. The first heating curves are displayed to show the effect of processing method, as well as the cooling curves and second heating curves. Glass transition (T_g), cold crystallization (T_{cc}), crystallization (T_c), and melting (T_m) temperatures were measured. The heat of fusion during cold crystallization (ΔH_{cc}), heat of crystallization (ΔH_c), and heat of fusion during melting (ΔH_f) were determined from the areas under the cold crystallization, crystallization, and melting peaks, respectively,

and normalized to the PTT content. Two specimens per concentration were tested and the average data reported.

Tensile Test. Tensile mechanical properties were determined using a MTS QTest/25 Elite Controller with a 5 kN load cell and extensometer (MTS model 632.11B-20 with a 1 inch gauge length) at a cross head speed of 5 mm/min, according to ASTM D 638 of Type I specimens with dimensions 3.4 mm x 12.5 mm x 165 mm (thickness x width x length). At least five specimens per sample were tested, and all error bars indicate standard deviation per sample. Modulus, ultimate tensile strength, percent strain at fracture, and total energy absorbed were calculated and the average of the five specimens reported.

Impact Test. Notched Izod impact resistance was determined using an Instron Dynatup POE 2000, according to ASTM D256 with an average impact velocity of 3.4 m/sec and 1.64 kg weight. Specimen dimensions were 3.4 mm x 12.5 mm x 63 mm (thickness x width x length). At least 10 specimens per sample were tested, and average impact resistance reported with error bars indicating standard deviation per sample.

RESULTS AND DISCUSSION

Morphology

The morphology of the FG-PTT PMC for 10%, 15%, 20%, and 30% FG in PTT is presented in Figures 3 and 4 at a 300 μm scale and 100 \times magnification. In Figure 3, the images were taken perpendicular to the machine direction and reveal good fiber distribution throughout the PTT matrix. In Figure 4, the images were taken parallel to the machine direction and reveal fiber orientation in the machine direction. In other words, the fibers appear to be pointing in the same direction. In Figure 5, images of 15 and 30 wt % FG in PTT were taken perpendicular to the machine direction at a 30 μm scale and 1000 \times magnification. The fiber–matrix gap spacing appears quite small and there is very little fiber-pull out, indicating good fiber–matrix bonding and near optimal fiber aspect ratio.

When fiber-pull out occurs and is dominant over fiber breakage, one may observe the fracture surface by eye or by optical microscope and see the fibers. Qualitatively, few short fibers were seen on the fracture surface of the FG-PTT composites produced using the novel method, as compared with long fibers visible on the fracture surface of FG-PTT composites prepared by standard processing methods in our labs. Good fiber–matrix bonding is required to allow load transfer between the reinforcing agent and the matrix and is evident in the mechanical property enhancement with increasing FG concentration.

Effect of FG Content and Processing Method on

Thermal Behavior

First heating, cooling, and second heating curves for one specimen of each FG-PTT composite are shown in Figure 6, and the tabulated results for T_g , T_{co} , ΔH_{co} , T_c , ΔH_c , T_m , and ΔH_f appear in Table I. In the first heat scan, the T_g , T_{co} , and T_m are independent of FG concentration and remain nearly constant at approximately 45°C, 66°C, and 227°C, respectively. Cold crystallization occurs for all concentrations, but ΔH_{cc} decreases with FG content. These values are similar to those found in the literature for neat PTT and clay-PTT nanocomposites.^{15,24} In the second

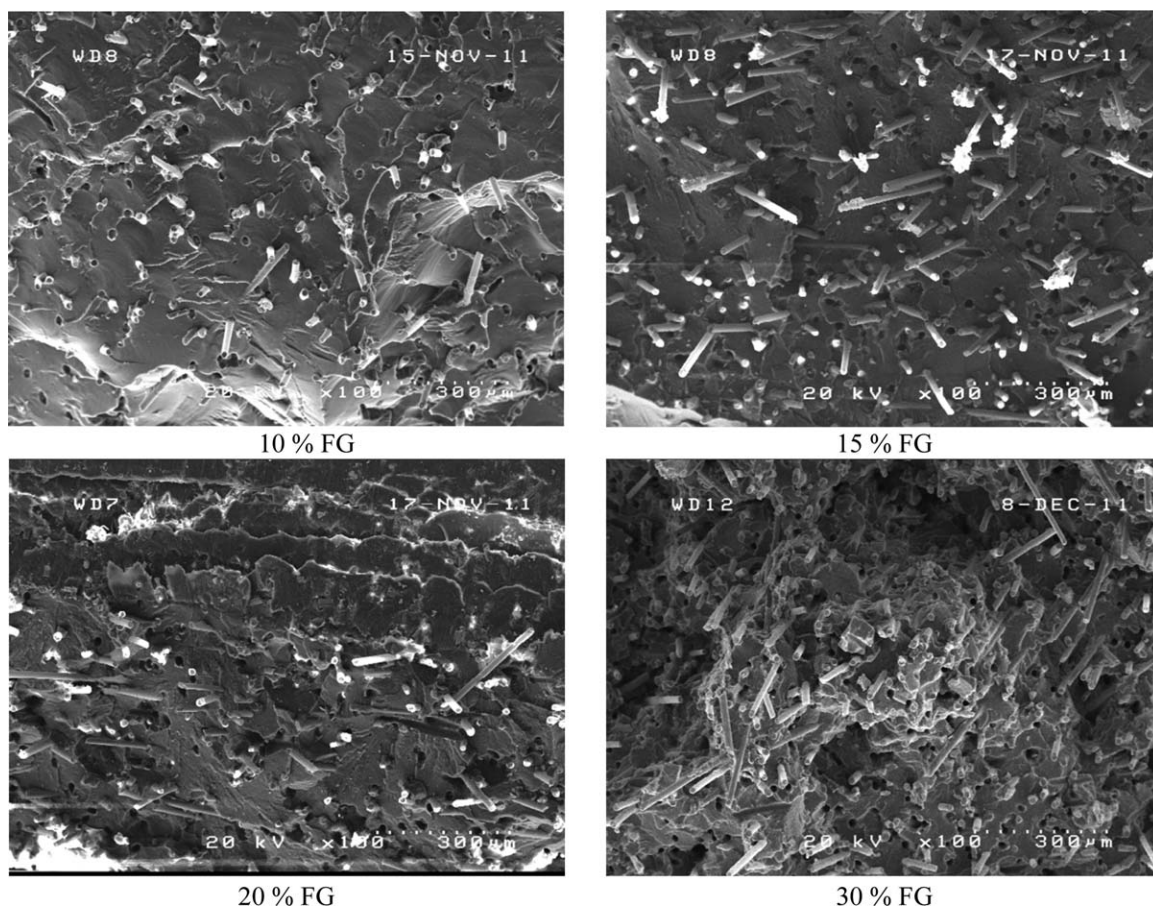


Figure 3. Morphology of the FG-PTT PMC by scanning electron microscopy at a 300 μm scale oriented perpendicular to the machine direction for 10, 15, 20, and 30 wt % FG in PTT.

heat scan, the T_g remains constant with the addition of FG to PTT at 52°C, which is 7°C higher than the first heat scan and cold crystallization does not occur. The T_m remains constant with addition of FG to PTT in both the first and second heat scans.

With addition of FG to PTT, the T_c values of all concentrations of the FG-PTT composites are elevated from the neat PTT value of 169°C to an average of 180°C. Similar to previous work, the increase in T_c with the addition of FG indicates that FG has a nucleating effect on PTT and an increase in crystallization rate.²² However after 10% FG in PTT, FG begins to hinder migration and diffusion of polymer molecular chains to the surface of the nucleus and T_c values no longer increase.²² In some cases, organoclays also act as nucleating agents and enhance crystallization rates of PTT.^{25–27} The degree of supercooling ($\Delta T = T_m - T_c$) decreases with the addition of FG, further supporting the notion that crystallization rate is higher for FG-PTT composites than for neat PTT.²⁵

The polymer crystallinity (X_c) is estimated from DSC measurements according to eq. (1), in which ΔH_f is the heat of fusion during melting, ΔH_{cc} is heat of fusion during cold crystallization, and ΔH_f° is the equilibrium heat of fusion of 100% crystalline PTT.^{28,29} For PTT, ΔH_f° is 30 kJ/mol.³⁰ The percent crystallinity of the as molded specimens is calculated from the first heat scan and appears in Table I. X_c increases with the

addition of FG to PTT, from 21.4% to 26.3% for neat PTT and 30% FG in PTT, respectively:

$$X_c = \frac{(\Delta H_f - \Delta H_{cc})}{\Delta H_f^\circ} \quad (1)$$

Effect of FG Content and Processing Method on Tensile Properties

Tensile stress–strain curves for 0%, 10%, 15%, 20%, and 30% FG in PTT appear in Figure 7, for which a representative curve from each sample is shown, and the corresponding data is shown in Table II. The 0% FG in PTT sample fractures on average at 178% strain and is not shown on the graph so that the scale is appropriate for the composites. With the addition of FG to PTT, the average values of tensile modulus and tensile strength increase, as shown in Table II and Figure 8. Surprisingly, % strain at fracture remains fairly constant with increasing FG concentration. Typically, % strain at fracture decreases with increasing chopped fiber content as the modulus increases and the composite becomes more brittle. The total energy absorbed until tensile strength increases with FG concentration. Thus, the FG-PTT PMC prepared using the novel method is stiff and strong while maintaining some ductility and offering enhanced toughness.

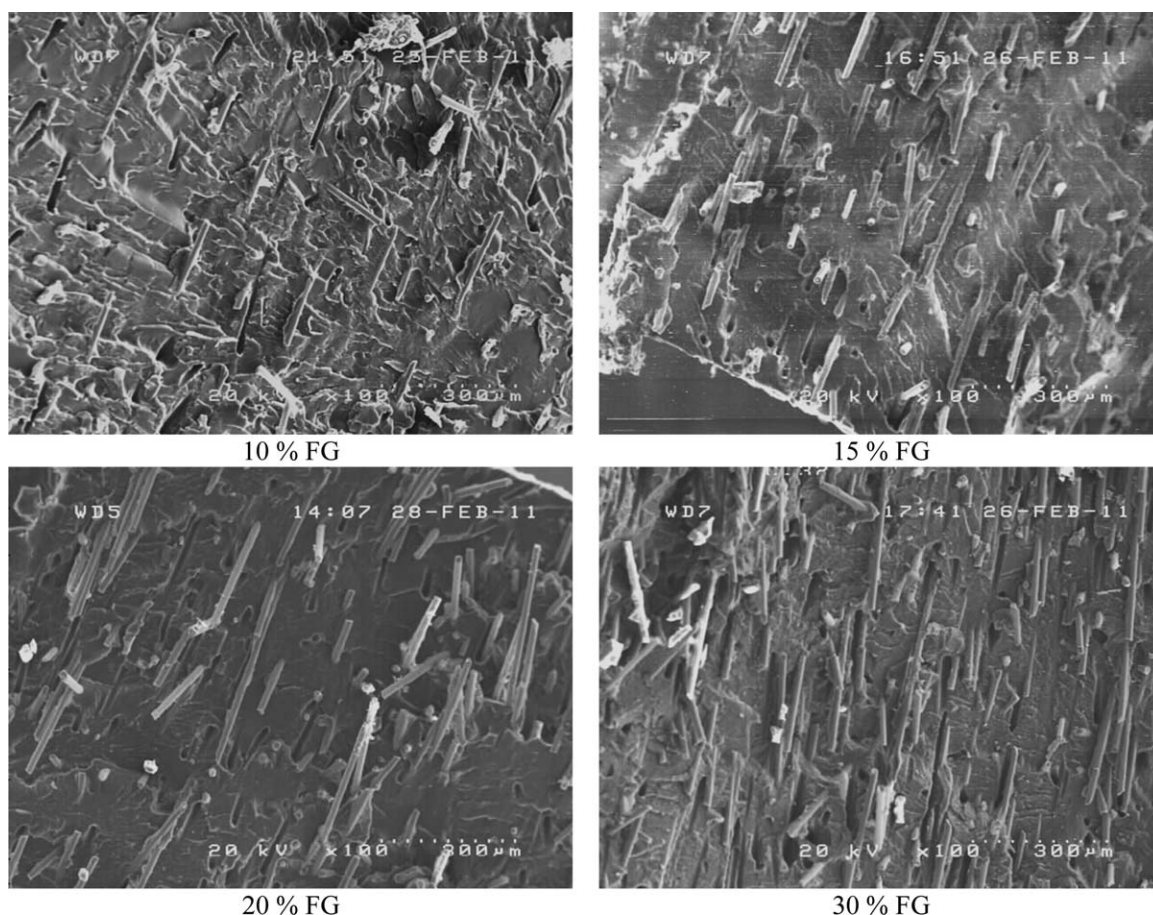


Figure 4. Morphology of the FG-PTT PMC by scanning electron microscopy at a 300 μm scale oriented parallel to the machine direction for 10, 15, 20, and 30 wt % FG in PTT.

These mechanical properties are similar to values found in the literature for an FG-PTT composite prepared by twin screw extrusion followed by injection molding using a mold temperature of 35°C for 0, 15, and 30% FG in PTT (unfilled data points),²² as shown with the novel processed composites (shaded data points) in Figure 8. However, tensile strength at 30% FG in

PTT prepared using this novel method is 20% higher than the composite shown in the literature prepared by twin screw extrusion followed by injection molding. This strength enhancement of the novel method is due to good fiber–matrix bonding and optimal fiber aspect ratio. Moreover, it has been shown that multiple processing steps cause degradation in PTT, resulting in

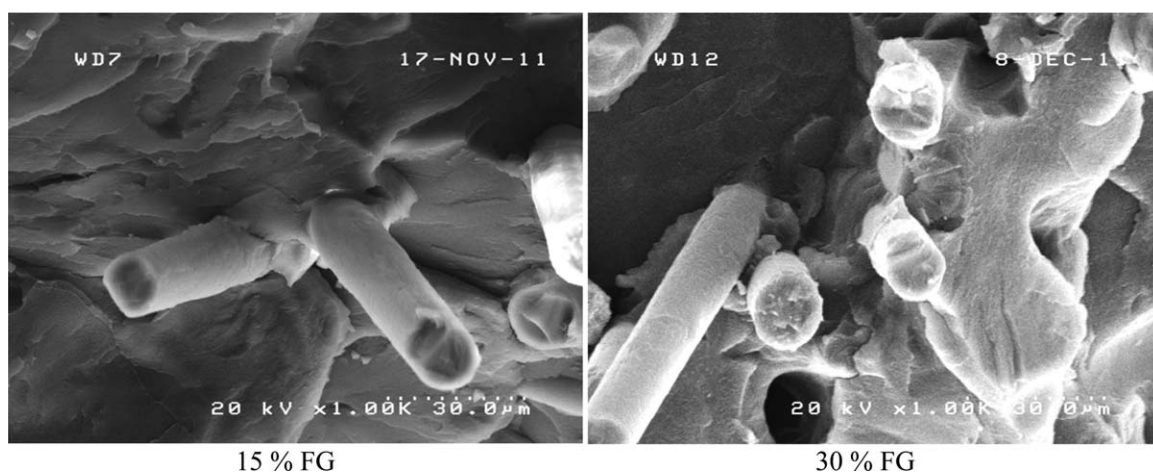


Figure 5. Detailed morphology of the FG-PTT PMC by scanning electron microscopy at a 30 μm scale oriented perpendicular to the machine direction for 15 and 30 wt % FG in PTT.

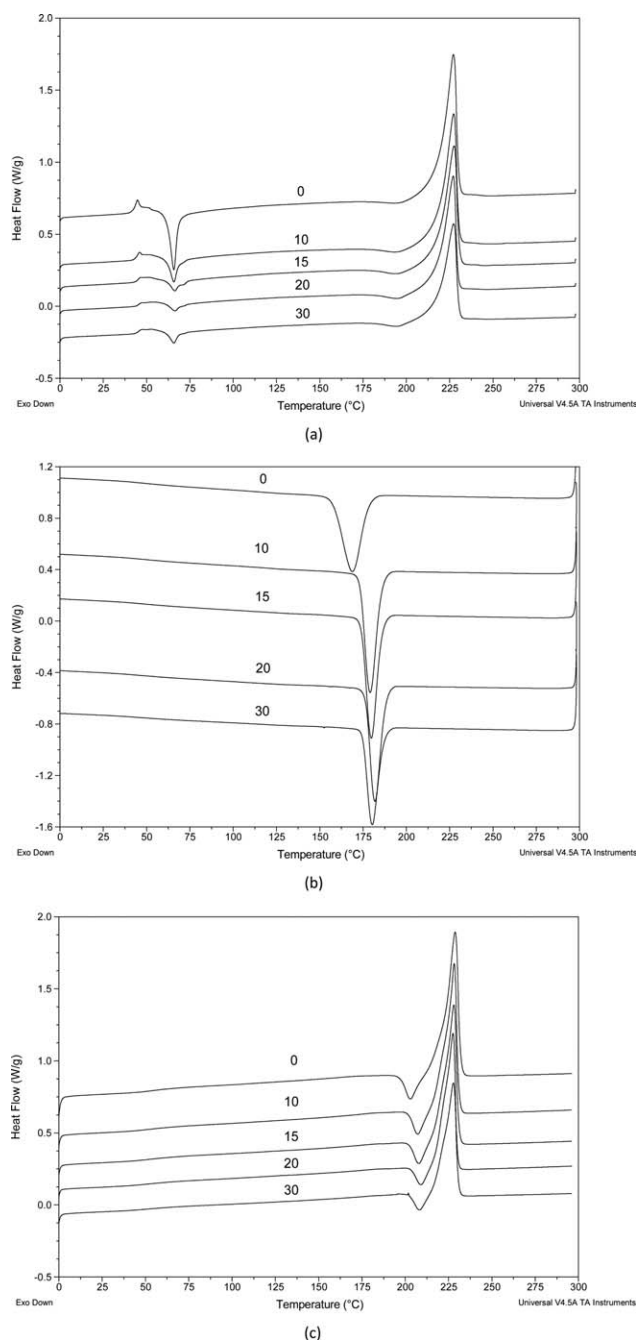


Figure 6. DSC thermograms at 10°C/min of 0%, 10%, 15%, 20%, and 30% FG in PTT: (a) first heat scans, (b) cooling scans, and (c) second heat scans.

Table I. Thermal Analysis Results Measured from DSC of 0%, 10%, 15%, 20%, and 30% FG in PTT

% FG	T_g (°C)		T_{cc} (°C)	ΔH_{cc} (kJ/mol)	T_c (°C)	ΔH_c (kJ/mol)	T_m (°C)		ΔH_f (kJ/mol)		ΔT (°C)	X_c (%)
	1 st Heat	2 nd Heat					1 st Heat	2 nd Heat	1 st Heat	2 nd Heat		
0	44	52	64	4.4	169	10.4	227	228	10.8	10.5	59	21.4
10	45	52	66	3.6	179	11.5	227	228	11.0	11.4	49	24.4
15	45	51	66	3.0	180	11.1	227	228	10.5	11.0	47	24.8
20	46	51	66	1.9	181	11.0	227	228	9.7	10.8	46	25.7
30	45	52	66	2.7	180	11.5	227	228	10.5	11.3	47	26.3

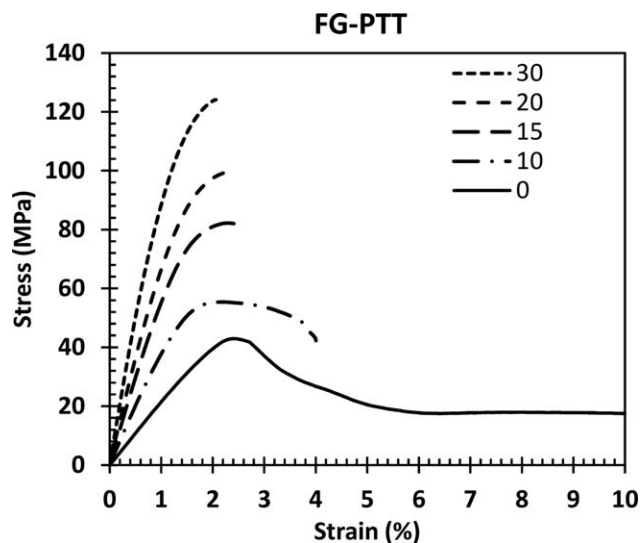


Figure 7. Average tensile stress–strain curves for 0, 10, 15, 20, and 30 wt % FG in PTT.

yellowing, molecular weight reduction, and decrease in tensile and impact break properties with each successive step.³¹ Thus, a one-step process that is able to compound and fabricate parts is highly desirable for this type of condensation polymer. Furthermore, mechanical property results, in conjunction with the morphology analysis, show that twin screw extrusion is not required to obtain good mixing (i.e. good dispersion and distribution of particles) and thus good mechanical properties for fiber-reinforced thermoplastic composites.

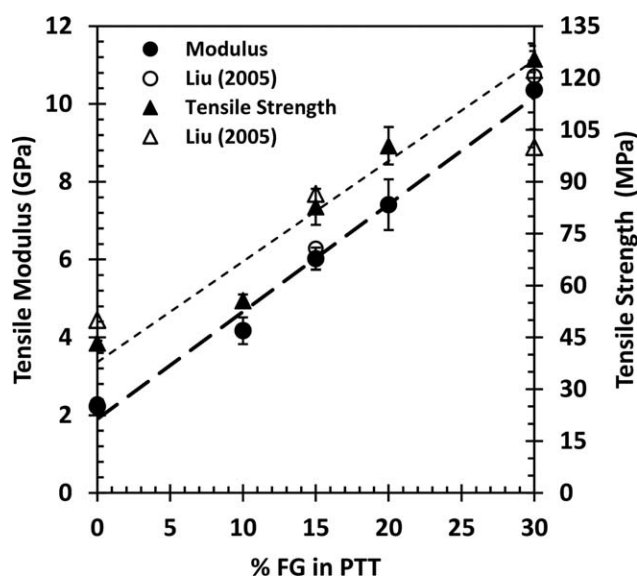
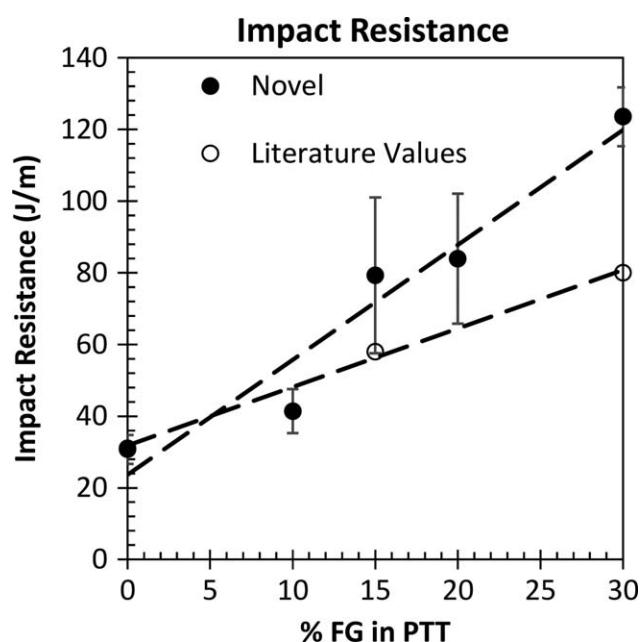
Tensile strength of 100% PTT is similar to values quoted in the literature when the mold temperature is 20°C; however, tensile strength is dependent upon the mold temperature used during processing.¹⁴ As the mold temperature increases, tensile strength of PTT also increases and is attributed to a simultaneous increase in the degree of crystallinity.¹⁴ Thus, tensile strength of PTT and FG-PTT composites is dependent upon processing method and mold temperature used during injection molding.

Effect of FG Content and Processing Method on Izod Impact Resistance

Average Izod impact resistance is shown in Figure 9 for the FG-PTT composite prepared using this novel method. Remarkably, impact resistance at 30% FG prepared using this novel method is 35% higher than values quoted in the literature,²² indicating superior fiber–matrix adhesion because of processing method.

Table II. Tensile Results of 0%, 10%, 15%, 20%, and 30% FG in PTT

% FG in PTT	Modulus (GPa)	Tensile Strength (MPa)	Strain at TS (%)	Energy Absorbed at TS (Nm)	Fracture Strength (MPa)	Strain at Fracture (%)
0	2.23	43	2.43	649	24	178
10	4.17	56	2.15	822	48	3.84
15	6.02	83	2.32	1376	83	2.31
20	7.41	100	2.47	1926	100	2.45
30	10.36	125	2.28	2111	125	2.25

**Figure 8.** Average tensile modulus and strength for 0%, 10%, 15%, 20%, and 30% FG in PTT.**Figure 9.** Notched Izod impact resistance for 0%, 10%, 15%, 20%, and 30% FG in PTT (shaded circle) compared to literature values (unfilled circle).

CONCLUSIONS

A successful one-step, novel injection molding processing method was developed and achieved a well-mixed FG-PTT composite with good fiber–matrix bonding. Thermal property results indicate that FG is an effective nucleating agent and increases the crystallization rates of PTT. Mechanical property results indicate that this novel method produces FG-PTT composites with enhanced ductility, toughness, and Izod impact resistance without sacrificing tensile modulus or tensile strength. Furthermore, at higher FG concentration, this FG-PTT composite offers superior strength and Izod impact resistance compared with values quoted in the literature.

The key advantages of this novel method include cost, time, and energy savings. Additionally, the novel method offers reduced fiber attrition and polymer degradation and enhanced mechanical properties. This novel method is applicable to polymer blends and other PMCs and will aid the polymer manufacturing industry by reducing the costs and energy required for traditional two-step pre-compounding followed by part fabrication methods.

ACKNOWLEDGMENTS

This work was supported by Rutgers University. Special acknowledgements to Thomas Nosker, Arya Tewatia, and Kendall Mills from Rutgers University and to Alexandra Todd from Washington and Lee University.

REFERENCES

- Canto, L. B.; Mantovani, G. L.; Covas, J. A.; Hage, E., Jr.; Pessan, L. A. *J. Appl. Polym. Sci.* **2007**, *104*, 102.
- Gale, M. *Adv. Polym. Technol.* **1997**, *16*, 251.
- Rios, A. T. C.; Osswald, T. A.; Noriega, M. P.; Estrada, O. A. Experimental study of various mixing sections in a single screw extruder, SPE-ANTEC Technical Papers, Conference Proceedings of the Society of Plastics Engineers ANTEC Conference, Atlanta, GA **1998**.
- Black, T. In *Plastics Compounding Equipment and Processing*; Todd, D., Ed.; Hanser Publishers: Cincinnati, **1998**; p 14.
- Luker, K. Summary Results of a Novel Single Screw Compounder, SPE-ANTEC Technical Papers, Conference Proceedings of the Society of Plastics Engineers ANTEC Conference, Cincinnati, OH, **2007**.

6. Luker, K.; Lynch, J. K.; Nosker, T. J. A novel micro-batch mixer that scales to a single screw compounder, SPE-ANTEC Technical Papers, Conference Proceedings of the Society of Plastics Engineers ANTEC Conference, Milwaukee, WI, **2008**.
7. Nosker, T. J.; Lynch, J. K.; Lehman, R.; Idol, J. D.; Renfree, R. W.; Renfree, M. US Patent 2013, 8,497,324.
8. Kurian, J. V. *J. Polym. Environ.* **2005**, *13*, 159.
9. Poulin-Dandurand, S.; Perez, S.; Revol, J. F.; Brisse, F. *Polymer* **1979**, *20*, 419.
10. Ho, R. M.; Ke, K. Z.; Chen, M. *Macromolecules* **2000**, 7529.
11. Wang, B.; Li, C. Y.; Hanzlicek, J.; Cheng, S. Z. D.; Geil, P. H.; Grebowicz, J.; Ho, R. M. *Polymer* **2001**, *42*, 7171.
12. Chuah, H. H. *Polym. Eng. Sci.* **2001**, *41*, 308.
13. Hong, P.; Chung, W.; Hsu, C. *Polymer* **2002**, *43*, 3335.
14. Zhang, J. *J. Appl. Polym. Sci.* **2004**, *91*, 1657.
15. Huang, J.; Ju, M.; Chu, P. P.; Chang, F. J. *Polym. Res.* **1999**, *6*, 259.
16. Ward, I. M.; Wilding, M. A.; Brody, H. J. *Polym. Sci. A-2 Polym. Phys.* **1976**, *14*, 263.
17. Shafee, E. E. *Polymer* **2003**, *44*, 3727.
18. Grebowicz, J. S.; Brown, H.; Chuah, H.; Olvera, J. M.; Wasiak, A.; Sajkiewicz, P.; Ziabicki, A. *Polymer* **2001**, *42*, 7153.
19. Wu, J.; Schultz, J. M.; Samon, J. M.; Pangelinan, A. B.; Chuah, H. H. *Polymer* **2001**, *42*, 7141.
20. Dangayach, K.; Chuah, H.; Gergen, W.; Dalton, P.; Smith, F. Poly (trimethylene terephthalate) - New opportunity in engineering thermoplastic applications, SPE-ANTEC Technical Papers, Conference Proceedings of the Society of Plastics Engineers ANTEC Conference, Toronto, Canada **1997**.
21. Farah, M.; Bretas, R. E. S. Rheological Characterization of Polyesters Based in Terephthates, SPE-ANTEC Technical Papers, Conference Proceedings of the Society of Plastics Engineers ANTEC Conference, San Francisco, CA, **2002**.
22. Liu, W.; Mohanty, A. K.; Drzal, L. T.; Misra, M.; Kurian, J. V.; Miller, R. W.; Strickland, N. *Ind. Eng. Chem. Res.* **2005**, *44*, 857.
23. Nosker, T. J.; Lynch, J. K.; Luker, K. Just-In-Time Compounding in an Injection Molding Machine, US Patent Application 20130072627 **2013**.
24. Hu, X.; Lesser, A. J. Morphological Studies on Poly (Trimethylene Terephthalate) (Ptt)/Clay Nanocomposites, SPE-ANTEC Technical Papers, Conference Proceedings of the Society of Plastics Engineers ANTEC Conference, San Francisco, CA, **2002**.
25. Ou, C. *J. Appl. Polym. Sci.* **2003**, *89*, 3315.
26. Ou, C. *J. Polym. Sci. B* **2003**, *41*, 2902.
27. Hu, X.; Lesser, A. J. *J. Polym. Sci. B* **2003**, *41*, 2275.
28. Murthy, N. S.; Khanna, Y. P.; Signorelli, A. J. *Polym. Eng. Sci.* **1994**, *34*, 1254.
29. Huang, J. M.; Chu, P. P.; Chang, F. C. *Polymer* **2000**, *41*, 1741.
30. Pyda, M.; Boller, A.; Grebowicz, J.; Chuah, H.; Lebedev, B. V.; Wunderlich, B. *J. Polym. Sci. B* **1998**, *36*, 2499.
31. Ramiro, J.; Eguiazbal, J. I.; Nazabal, J. *J. Appl. Polym. Sci.* **2002**, *86*, 2775.